

See discussions, stats, and author profiles for this publication at: <https://www.researchgate.net/publication/43347340>

Development of a Selective Modulator of Aryl Hydrocarbon (Ah) Receptor Activity that Exhibits Anti-Inflammatory Properties

ARTICLE *in* CHEMICAL RESEARCH IN TOXICOLOGY · MAY 2010

Impact Factor: 3.53 · DOI: 10.1021/tx100045h · Source: PubMed

CITATIONS

37

READS

46

9 AUTHORS, INCLUDING:



Krishnegowda Gowdahalli

Pennsylvania State University

36 PUBLICATIONS 977 CITATIONS

SEE PROFILE



Chris Richard Chiaro

Pennsylvania State University

20 PUBLICATIONS 397 CITATIONS

SEE PROFILE



Arun K Sharma

Penn State Hershey Medical Center and Pen...

138 PUBLICATIONS 1,522 CITATIONS

SEE PROFILE



Gary H Perdew

Pennsylvania State University

150 PUBLICATIONS 6,623 CITATIONS

SEE PROFILE

Published in final edited form as:

Chem Res Toxicol. 2010 May 17; 23(5): 955–966. doi:10.1021/tx100045h.

Development of a Selective Modulator of Aryl Hydrocarbon (Ah) Receptor Activity that Exhibits Anti-Inflammatory Properties

Iain A. Murray[†], Gowdahalli Krishnegowda[¶], Brett C. DiNatale[†], Colin Flaveny[†], Chris Chiaro[†], Jyh-Ming Lin[§], Arun K. Sharma[¶], Shantu Amin[¶], and Gary H. Perdew^{†,*}

[†]Department of Veterinary and Biomedical Sciences and Center for Molecular Toxicology and Carcinogenesis, The Pennsylvania State University, University Park, Pennsylvania, 16802

[¶]Department of Pharmacology, Penn State College of Medicine, Hershey, Pennsylvania 17033

[§]Department of Biochemistry and Molecular Biology, Penn State College of Medicine, Hershey, Pennsylvania 17033

Abstract

The aryl hydrocarbon receptor (AHR) is a ligand-activated transcription factor that mediates the toxicity of 2,3,7,8-tetrachlorodibenzo-*p*-dioxin. However, the role of the AHR in normal physiology is still an area of intense investigation. For example, this receptor plays an important role in certain immune responses. We have previously determined that the AHR can mediate repression of acute-phase genes in the liver. For this observation to be therapeutically useful, selective activation of the AHR would likely be necessary. Recently, the selective estrogen receptor ligand WAY-169916 has also been shown to be a selective AHR ligand. WAY-169916 can efficiently repress cytokine-mediated acute-phase gene expression (e.g. *SAA1*), yet fail to mediate a dioxin response element-driven increase in transcriptional activity. The goals of this study were to structurally modify WAY-169916 to block binding to the estrogen receptor and increase its affinity for the AHR. A number of WAY-169916 derivatives were synthesized and subjected to characterization as AHR ligands. The substitution of a key hydroxy group for a methoxy group ablates binding to the estrogen receptor and increases its affinity for the AHR. The compound 1-allyl-7-trifluoromethyl-1H-indazol-3-yl]-4-methoxyphenol (SGA 360), in particular, exhibited essentially no AHR agonist activity, yet was able to repress cytokine-mediated *SAA1* gene expression in Huh7 cells. SGA 360 was tested in a 12-O-tetradecanoylphorbol-13-acetate (TPA)-mediated ear inflammatory edema model using C57BL6/J and *Ahr*^{-/-} mice. Our findings indicate that SGA 360 significantly inhibits TPA-mediated ear swelling and induction of a number of inflammatory genes (e.g. *Saa3*, *Cox2*, *Il6*) in C57BL6/J mice. In contrast, SGA 360 had no effect on TPA-mediated ear swelling or inflammatory gene expression in *Ahr*^{-/-} mice. Collectively, these results indicate that SGA 360 is a selective Ah receptor modulator (SAhRM) that exhibits anti-inflammatory properties in vivo.

Introduction

An important aspect of systemic inflammation is the induction of an acute phase response in the liver. Circulating cytokines such as TNF α or IL1 β are elevated during sepsis or chronic

*To whom correspondence should be addressed. CMTC, 309 LSB, The Pennsylvania State University, University Park, PA Phone: 814-865-0400; Fax: 814-863-1696; ghp2@psu.edu.

Supporting Information Available: Copies of the ¹H NMR spectra for compounds **1**, **2**, **3**, **4**, **5**, **10**, **11**, **12**, **13**, and **14**. Copies of ¹³C NMR spectra (Figures S1 and S2) and partial HMBC spectra (Figures S3 and S4) for compound **4** and **14** are available. Figures S5 and S6 provide additional data demonstrating that SGA 360 does not interact with the ER. This material is available free of charge via the internet at <http://pubs.acs.org>.

inflammatory diseases. Inflammatory signaling within hepatocytes results in the induction of a series of genes that includes C-reactive protein, LPS binding protein, complement C3, tissue plasminogen activator and serum amyloid A (SAA) (1). There are four members of this latter gene family in rodents, *Saa1* through 4. With *Saa1* and *Saa2* being the primary genes that contribute to the inducible circulating pool of SAA in serum. The induction of an acute phase response is generally believed to be an adaptive response in the short term that aids in the reaction to infection and other inflammatory insults. SAA has been suggested as an excellent marker for systemic inflammation, in part because up to a 1000-fold increase in transcription of these genes has been observed. However, recent studies of the biological activity of SAA suggest that it may also be a mediator of inflammation. SAA binds to FPRL1, RAGE and TLR2 receptors; activation of these receptors leads to enhanced inflammatory signaling through activation of NF κ B and AP1 (2–4). Prolonged production of SAA can lead to an array of adverse effects, such as accumulation of fibrils leading to amyloidosis (5). Therefore, repression of the acute phase response in liver would be an important therapeutic target for a diverse array of chronic inflammatory diseases.

The AHR is a ligand activated basic-helix-loop-helix/Per-ARNT-Sim transcription factor that is responsible for the toxicity of TCDD (commonly referred to as dioxin). Upon ligand binding, the AHR, bound to hsp90, translocates into the nucleus where ARNT displaces hsp90 and heterodimerizes with the AHR (6). The ligand-bound AHR/ARNT complex is then able to bind to a dioxin responsive element (DRE) in the promoter of a wide range of genes involved in drug metabolism (e.g. *Cyp1a1*) as well as growth and metabolism (e.g. *Ereg*, *Snai2*). The physiological role of the AHR continues to be an active area of investigation and was first explored through examination of the phenotype of *Ahr* null mice. These mice exhibit a number of defects, such as immune system dysfunction, poor liver vasculature development, and reduced fecundity (7). This latter phenotype appears to be due to multiple defects that result in lower conception rate, smaller litter size and low pup survival rates (8). The lack of AHR expression alters maturation of follicles apparently due to a lack of estradiol synthesis (9). Cardiovascular effects, such as a systemic hypertension and hypoxemia condition, have been observed in *Ahr* null mice, dependent on the altitude (10).

Perhaps the area of AHR biology that has received the most recent attention is the ability of the AHR to influence T cell differentiation. The AHR can play a role in the balance of T_H1 and T_H2 cells, this was established through the use of an AHR agonist M50367 that mediates a preference for increased T_H1 versus T_H2 cells (11,12). M50367 exposure in mice leads to a decreased response in an allergic experimental model. Differentiation of naïve T-cells leads to enhanced AHR expression and supports the concept that the AHR mediates key steps in this process. Interleukin 17 (IL17)-producing T helper cells (Th17) are a proinflammatory subset of T helper cells that play a critical role in the experimental development of autoimmune diseases, such as collagen-induced arthritis (13). The AHR plays an important role in the development of Th17 cells in both in vitro and in vivo experimental models (14,15). Furthermore, the AHR appears to regulate STAT1 activation during T cell differentiation into Th17 cells (16). How the AHR activation occurs under physiologic conditions is unknown, and whether these effects are mediated by endogenous ligands remains to be determined.

There are numerous reports indicating that prolonged activation of the AHR via exposure to high levels of an AHR agonist leads to enhanced inflammatory signaling (17). However, more recent studies have revealed that the AHR can mediate anti-inflammatory responses as well, through interference with NF κ B signaling or repression of *IL6* induction (18,19). We have recently demonstrated that the AHR can attenuate cytokine-mediated induction of the acute phase response gene expression in liver (20). This appears to be a selective response considering that the AHR fails to influence the induction of *Il8* or *Nfkb*. However, sustained activation of the AHR by xenobiotic agonists can lead to toxicity through a predominantly

dioxin responsive element-mediated mechanism (21). Therefore, we tested the hypothesis that the AHR could be selectively activated by an appropriate ligand to repress cytokine-mediated induction of the acute phase response, yet fail to significantly induce gene expression through binding to its cognate response element. This goal was accomplished through the identification of the selective estrogen receptor ligand, WAY-169916, as a selective² AHR modulator³ (SAhRM) (22). However, because of the dual AHR/estrogen receptor (ER) specificity of this compound, there is a need to find compounds that exhibit enhanced selectivity for the AHR. In this report structure-activity studies were performed to modify the structure of WAY-169916 in order to enhance its affinity for the AHR and increase its AHR-mediated efficacy following modification. The following properties of the AHR were examined: to maintain SAhRM potential (i.e. mediate *Saa1* gene repression) in the absence of DRE-mediated signaling; to exhibit cross-species SAhRM activity; and to diminish or ablate ER binding status. One compound was synthesized, SGA 360, which met all of these criteria and proved useful in selectively modulating AHR activity in vivo.

Materials and Methods

Chemistry

Melting points were recorded on a Fischer-Johns melting point apparatus and are uncorrected. NMR spectra were recorded using a Bruker Avance 500 MHz spectrometer. Chemical shifts were recorded in ppm downfield from the internal standard. The signals are quoted as s (singlet), d (doublet), t (triplet), m (multiplet) and dt (doublet of triplet). MS analysis were run on a Hewlett-Packard Model 5988A instrument. Thin-layer chromatography (TLC) was developed on aluminum-supported pre-coated silica gel plates (EM industries, Gibbstown, NJ). Column chromatography was conducted on silica gel (60–200 mesh). The indazole derivatives were synthesized by following a previously described method with minor modifications (23) as detailed below:

Synthesis of 2-fluoro-N-methoxy-N-methyl-3-(trifluoromethyl)benzamide, 9—To a solution of 2-fluoro-3-(trifluoromethyl)benzoic acid (Compound **6**, 5.0 g, 24.02 mmol) in anhydrous tetrahydrofuran (THF) (100 ml) were added 2-chloro-4,6-dimethoxy-1,3,5-triazine (Compound **7**, 5.06 g, 28.81 mmol) and *N*-methylmorpholine (7.92 ml, 72.06 mmol). A white precipitate was formed at room temperature during stirring 1 h, and then *N,O*-dimethylhydroxylamine hydrochloride (2.5 g, 24.02 mmol) was added. The mixture was stirred at room temperature for additional 8 h, quenched with water (50 ml), and extracted with ethyl acetate (3 × 100 ml). The combined organic layers were washed with saturated solution of sodium carbonate, followed by 1 N hydrochloric acid, and brine. The organic layer was dried over anhydrous sodium sulfate and evaporated *in vacuo* to yield **9** (5.2 g, 86%) as a viscous oil. ¹H NMR (500 MHz, CDCl₃) δ 7.72–7.31 (m, 3H), 3.56 (s, 3H), 3.39 (s, 3H); ESI-MS 252 [M+H]⁺.

Synthesis of 2,4-dimethoxyphenyl[(2-fluoro-3-(trifluoromethyl)phenyl)methanone, 10—2,4-Dimethoxyphenylmagnesium bromide (60 ml, 0.5M in THF, 29.88 mmol) was added to a solution of compound **9** (2.5 g, 9.96 mmol) in anhydrous THF (50 ml) at 0 °C. The reaction mixture was stirred for 2 h at 0 °C and quenched with 5% hydrochloric acid in ethanol (20 ml). The solvents were removed under reduced pressure, extracted with ethyl acetate, washed with water, dried over anhydrous magnesium sulfate and evaporated *in vacuo*. The crude product was purified by silica gel column chromatography, using ethyl

²The term “selective” is used to describe an AHR (or ER) ligand that exhibits a subset of altered transcriptional activities. The term is not used to infer that a given AHR ligand does not interact with other proteins.

³A SAhRM is defined as an AHR ligand that is not capable of mediating a dioxin responsive element driven transcription. Yet is able to mediate other activities such as repression of cytokine mediated acute-phase gene expression.

acetate/hexanes (1:9) as eluent, to obtain **10** (2.6 g, 81%) as a white solid; mp 78–80 °C; ¹H NMR (500 MHz, CDCl₃) δ 7.84–7.71 (m, 3H), 7.34 (t, 1H, *J* = 7.5 Hz), 6.61 (dd, 1H, *J* = 2.5 and 9.0 Hz), 6.46 (d, 1H, *J* = 2.5 Hz), 3.90 (s, 3H), 3.64 (s, 3H); ESI-MS 329 [M+H]⁺.

Synthesis of 3,4-dimethoxyphenyl[(2-fluoro-3-(trifluoromethyl)phenyl]

methanone, 11—Following an identical procedure and purification as described above for **10**, using 3,4-dimethoxyphenylmagnesium bromide gave **11** (2.4 g, 75%) as a white solid; mp 101–103 °C; ¹H NMR (500 MHz, CDCl₃) δ 7.79–7.82 (m, 1H), 7.71–7.74 (m, 1H), 7.57 (d, 1H, *J* = 2.0 Hz), 7.40 (t, 1H, *J* = 7.5 Hz), 7.30 (dt, 1H, *J* = 8.5 and 2.0 Hz), 6.91 (d, 1H, *J* = 8.5 Hz), 3.98 (s, 3H), 3.97 (s, 3H); ESI-MS 329 [M+H]⁺.

Synthesis of 3-(2,4-dimethoxyphenyl)-7-(trifluoromethyl)-1H-indazole, 12—To a solution of compound **10** (2.0 g, 6.09 mmol) in anhydrous pyridine (20 ml) was added anhydrous hydrazine (0.29 g, 9.0 mmol) and the reaction mixture was irradiated in a microwave apparatus for 1 h at 250W, 100 °C. The solvent was evaporated under reduced pressure, extracted with ethyl acetate, washed with water, dried over anhydrous sodium sulfate and concentrated to provide product **12** (1.85 g, 94%) as a white solid; mp 134–136 °C; ¹H NMR (500 MHz, DMSO-*d*₆) δ 13.58 (s, 1H), 7.91 (d, 1H, *J* = 8.0 Hz), 7.74 (d, 1H, *J* = 7.5 Hz), 7.46 (d, 1H, *J* = 8.0 Hz), 7.27 (t, 1H, *J* = 7.5 Hz), 6.77 (d, 1H, *J* = 2.0 Hz), 6.69–6.66 (m, 1H), 3.86 (s, 3H), 3.80 (s, 3H); ESI-MS 322.9 [M+H]⁺.

Synthesis of 3-(3,4-dimethoxyphenyl)-7-(trifluoromethyl)-1H-indazole, 13—

Microwave irradiation of compound **11** under identical conditions as described above for **12** yielded product **13** (1.83 g, 93%) as a white solid; mp 175–177 °C; ¹H NMR (500 MHz, DMSO-*d*₆) δ 8.36 (d, 1H, *J* = 8.0 Hz), 7.80 (d, 1H, *J* = 7.0 Hz), 7.53 (dd, 1H, *J* = 8.0 and 2.0 Hz), 7.49 (d, 1H, *J* = 2.0 Hz), 7.37 (t, 1H, *J* = 7.5 Hz), 7.13 (d, 1H, *J* = 8.5 Hz), 3.88 (s, 3H), 3.84 (s, 3H); ESI-MS 322.9 [M+H]⁺.

Synthesis of 1-allyl-3-(2,4-dimethoxyphenyl)-7-(trifluoromethyl)-1H-indazole, 2 and 2-allyl-3-(2,4-dimethoxyphenyl)-7-(trifluoromethyl)-2H-indazole, 3—Sodium hydride (60% in oil, 0.21 g, 5.12 mmol) was added slowly to a solution of Compound **12** (1.5 g, 4.66 mmol) in anhydrous *N,N*-dimethylformamide (15 ml) at room temperature. The reaction mixture was stirred for 30 minutes at ambient temperature to 60 °C. Allyl bromide (1.36 g, 11.26 mmol) was then added and the reaction mixture was stirred for an additional 4 h at 60 °C. The mixture was poured into ice cold water, the solid product was separated by filtration, washed with water and the isomers were purified by silica gel column chromatography eluting with 1% ethyl acetate in hexanes to provide products **2** [0.68 g (40%); mp 96–98 °C; ¹H NMR (500 MHz, CDCl₃) δ 7.88 (d, 1H, *J* = 8.0 Hz), 7.73 (d, 1H, *J* = 7.0 Hz), 7.50–7.48 (m, 1H), 7.16 (t, 1H, *J* = 7.5 Hz), 6.63–6.61 (m, 2H), 6.13–6.08 (m, 1H), 5.19 (d, 2H, *J* = 11.5 Hz), 5.16 (dd, 1H, *J* = 6.5 and 8.0 Hz), 5.06 (dd, 1H, *J* = 1.5 and 17 Hz), 3.87 (s, 3H), 3.80 (s, 3H)]; ESI-MS 363 [M+H]⁺; and **3** [0.51 g (30%); mp 73–75 °C; ¹H-NMR (500 MHz, CDCl₃) δ 7.60 (d, 2H, *J* = 7.5 Hz), 7.22 (d, 1H, *J* = 8 Hz), 7.05 (t, 1H, *J* = 7.5 Hz), 6.65–6.61 (m, 2H), 6.05–5.99 (m, 1H), 5.11 (dd, 1H, *J* = 1.5 and 10 Hz), 5.02–4.92 (m, 3H), 3.90 (s, 3H), 3.75 (s, 3H)]; ESI-MS 363 [M+H]⁺; as white solids.

Synthesis of 1-allyl-3-(3,4-dimethoxyphenyl)-7-(trifluoromethyl)-1H-indazole, 4 and 2-allyl-3-(3,4-dimethoxyphenyl)-7-(trifluoromethyl)-2H-indazole, 14—

Subjecting compound **13** to identical reaction conditions as described above for compound **12** in the synthesis of **2** and **3**, yielded products **4** [0.76 g (45%), viscous oil]; ¹H NMR (500 MHz, CDCl₃) δ 8.21 (d, 1H, *J* = 7.5 Hz), 7.80 (d, 1H, *J* = 7.5 Hz), 7.47–7.44 (m, 2H), 7.27 (t, 1H, *J* = 7.5 Hz), 7.04 (d, 1H, *J* = 8.0 Hz), 6.16–6.09 (m, 1H), 5.25–5.23 (m, 2H), 5.21 (dd, 1H, *J* = 10.5 and 1.5 Hz), 5.07 (dd, 1H, *J* = 17.0 and 1.5 Hz), 4.02 (s, 3H), 3.98 (s, 3H)]; ESI-MS

363 [M+H]⁺; and **14** [0.56 g (33%); mp 86–88 °C; ¹H-NMR (500 MHz, CDCl₃) δ 7.77 (d, 1H, *J* = 8.5 Hz), 7.67 (d, 1H, *J* = 7.0 Hz), 7.15–7.10 (m, 2H), 7.06 (d, 1H, *J* = 8.5 Hz), 7.03 (d, 1H, *J* = 2.0 Hz), 6.23–6.14 (m, 1H), 5.28 (dd, 1H, *J* = 10.0 and 1.0 Hz), 5.13–5.11 (m, 2H), 5.06 (dd, 1H, *J* = 17.5 and 1.0 Hz), 4.01 (s, 3H), 3.93 (s, 3H)]; ESI-MS 363 [M+H]⁺, as white solids.

Synthesis of 4-[1-allyl-7-trifluoromethyl-1H-indazol-3-yl]benzene-1,3-diol, 1—To a solution of Compound **8** (0.5 g, 0.38 mmol) in 5 ml of methylene chloride/cyclohexane (6:1) was added boron tribromide (1.0 M in methylene chloride, 11.02 ml, 11.04 mmol) at –30 °C. The reaction was allowed to warm to room temperature over 5 h. The reaction was quenched with 2 ml methanol and diluted with methylene chloride. The organic phases were washed with saturated sodium bicarbonate solution, dried over anhydrous sodium sulfate and concentrated *in vacuo*. The residue was purified by silica gel column chromatography eluting with 1% methanol in methylene chloride to obtain product **10** (210 mg, 45%) as a white solid, mp 113–115 °C; ¹H NMR (500 MHz, acetone-*d*₆) δ 8.55 (d, 1H, *J* = 8.5 Hz), 7.96 (d, 1H, *J* = 7.5 Hz), 7.93 (d, 1H, *J* = 8.5 Hz), 7.44 (t, 1H, *J* = 8 Hz), 6.57 (dd, 1H, *J* = 2.5 and 8.5 Hz), 6.54 (d, 1H, *J* = 2.5 Hz), 6.16–6.09 (m, 1H), 5.23–5.18 (m, 3H), 5.05 (dd, 1H, *J* = 1.5 and 17 Hz); ESI-MS 335 [M+H]⁺.

Synthesis of 2-[1-allyl-7-trifluoromethyl-1H-indazol-3-yl]-4-methoxyphenol, 5—Following an identical procedure and purification as described above for **1**, except for using 1 equivalent (0.38 mmol) boron tribromide gave **5** (0.22 g, 47%) as a white solid; mp 52–54 °C; ¹H-NMR (500 MHz, Acetone-*d*₆) δ 8.59 (d, 1H, *J* = 8.5 Hz), 8.03 (d, 1H, *J* = 8.5 Hz), 7.99 (d, 1H, *J* = 7.5 Hz), 7.47 (t, 1H, *J* = 8.0 Hz), 6.68 (dd, 1H, *J* = 8.5 and 2.5 Hz), 6.64 (d, 1H, *J* = 2.5 Hz), 6.21–6.12 (m, 1H), 5.27 (d, 1H, *J* = 5.5 Hz), 5.23 (dd, 1H, *J* = 10.5 and 1.0 Hz), 5.07 (dd, 1H, *J* = 17.0 and 1.0 Hz), 3.87 (s, 3H); ESI-MS 349 [M+H]⁺.

Biology. ERα competition assay

The ER-α Competitor Assay, Green (Invitrogen) was performed following manufacturer's instructions. Briefly, compounds and DMSO vehicle were diluted to twice their final assay concentrations in PanVera supplied ES2 screening buffer and added to 60 × 150 mm borosilicate glass cell culture tubes. A master mix was made of screening buffer with human recombinant ERα added, for a final concentration of 6 pmol/μl, and ES2 fluoromone added, for a final concentration of 400 nM. The master mix was added to diluted test compounds in a 1:1 volume, mixed gently, and incubated in the dark at room temperature for 2 h. Samples were then measured for fluorescence polarization using the PanVera Beacon 2000 polarization instrument with 485 nm excitation and 530 nm emission filters at 25° C. Results shown are the mean of samples performed in triplicate.

Cell Culture

All cell lines utilized except MCF-7 cells were maintained in modified Eagle's α-minimum essential medium (Sigma), supplemented with 1000 units/ml penicillin, 100 ug/ml streptomycin (Sigma), and 8% fetal bovine serum (Hyclone) under standard conditions. Huh 7 cells were obtained from Curt Omiecinski (Penn State University). MCF-7 cells were obtained from ATCC.

Cell-based Luciferase Reporter Assays

The DRE-driven luciferase reporter cell lines, human HepG2 40/6 and mouse H1L1.1c2, were used to assess AHR transcriptional activity (24,25). The latter cell line was kindly provided by Michael Denison (Univ. of CA, Davis). Luciferase activity was measured using the Promega Luciferase Assay system (Madison, WI).

Quantitation of mRNA Levels

Total RNA was isolated from cells using TRI reagent (Sigma) following manufacturer's standard protocol and converted to cDNA using a High Capacity cDNA Archive Kit from Applied Biosystems. The levels of *CYP1A1* and *SAA1* were determined by real-time qPCR using iQ SYBR Green supermix reagent (BioRad) and a MyIQ single-color PCR detection system (Bio-Rad). Primer sequences utilized have been previously described or are listed below (19). PCR primers (Integrated DNA Technologies, Coralville, IA) used in this study are as follows human *L13a* (forward) CCTGGAGGAGAAGAGGAAAGAGA, human *L13a* (reverse) GAGGACCTCTGTGTATTTGTCAA; human *SAA1* (forward) AGGCTCAGACAAATACTTCCATGC, human *SAA1* (reverse) TCTCTGGCATCGCTGATCACTTCT; human *CYP1A1* (forward) TCTTCCTTCGTCCCCTTCAC, human *CYP1A1* (reverse) TGGTTGATCTGCCACTGGTT; mouse *Il1b* (forward) ATACTGCCTGCCTGAAGCTCTTGT, mouse *Il1b* (reverse) AAGGGCTGCTTCCAAACCTTTGAC; mouse *Saa3* (forward) ATGCCAGAGAGGCTGTCCAGAAGT, mouse *Saa3* (reverse) TATCTTTTAGGCAGGCCAGCAGGT; mouse *L13a* (forward) TTCGGCTGAAGCCTACCAGAAAGT, mouse *L13a* (reverse) GCATCTTGGCCTTTTCCGTT; mouse *Cox2* (FORWARD) TTGCTGTACAAGCAGTGGCAAAGG, mouse *Cox2* (REVERSE) TGCAGCCATTTCTTCTCTCCTGT; mouse *Il10* (FORWARD) TGAATCCCTGGGTGAGAAGCTGA, mouse *Il10* (REVERSE) TGGCCTTGTAGACACCTTCCTCTT. In all cases, melting point analysis revealed amplification of a single product. Data acquisition and analysis were achieved using MyIQ software (Bio-Rad, Hercules, CA). Quantification was achieved through comparison against target-specific standard curves and data represent mean fluorescence normalized to that of the control gene ribosomal protein *L13a* to yield a relative mRNA level.

AHR Competition Binding Assay

The AHR photoaffinity ligand 2-azido-3-[¹²⁵I]-7,8-dibenzo-*p*-dioxin was synthesized as described (26). Liver cytosolic extract from B6.Cg-Ahr^{tm1Bra}Tg (Alb-cre, Ttr-AHR)1Ghp (express the human AHR in hepatocytes) was utilized in a photoaffinity ligand competition binding assay as previously described (27,28).

Electrophoretic Mobility Shift Assay (EMSA)

DRE-specific EMSAs were performed using in vitro translated human AHR and ARNT as previously described (28).

SAA Repression Assay

Huh7 cells were treated with SGA compounds for 1 h prior to the addition of 2 ng/ml of IL1B for 6 h. RNA was isolated and *SAA1* mRNA levels determined as previously described (20).

In vivo ear edema model

Ear inflammation was induced in anesthetized 6 week-old male C57BL6/J mice (wild-type or *Ahr*^{-/-}) through topical application of 1.5 µg 12-O-tetradecanoylphorbol-13-acetate (TPA) in 50 µl vehicle (HPLC-grade acetone) (Sigma) to the right ear. Anti-inflammatory properties of SGA 360 were examined through topical application of 30 µg SGA 360 in 50 µl vehicle immediately followed by administration of TPA. In all cases the left ear received vehicle alone. Six hours after induction of inflammation animals were euthanized by carbon dioxide asphyxiation and the degree of inflammation was assessed. Edema thickness was measured using a micrometer and edema weight was determined following isolation of a 7 mm ear punch. Total RNA was isolated from ear punches and RNA concentration was determined via

spectrophotometry at λ 260 nm and 280 nm. Total RNA was reverse transcribed to cDNA using a High Capacity cDNA Archive Kit (Applied Biosystems, Foster City, CA).

Statistical analysis

One-way ANOVA was followed by Tukey's Multiple Comparison Test was used to compare treatments using GraphPad Prism v5.0.

Results

Synthesis of indazole derivatives

The synthesis of indazole derivatives **1–5** was carried out as outlined in Scheme 1. The amide **9** was synthesized from 2-fluoro-3-(trifluoromethyl)benzoic acid following literature methods (29,30). Conversion of compound **9** to benzophenone derivative **10** was accomplished by treating it with 2,4-dimethoxyphenylmagnesium bromide. Microwave irradiation of **10** in the presence of anhydrous hydrazine gave an excellent yield (94%) of compound **12**, which, on treatment with allyl bromide in the presence of sodium hydride, resulted in a mixture of desired indazole derivatives **2** and **3**. A similar reaction sequence led to the formation of a mixture of compounds **4** and **14**. The two isomers in each case were separated by silica gel column chromatography. The compound **1** (WAY-169916) was obtained by treating compound **2** with excess of boron tribromide, while selective demethylation of **2** using 1 equivalent of boron tribromide led to an exclusive formation of monohydroxy derivative **5**.

The structures of 1-allyl and 2-allyl substituted isomers **4** and **14** are similar and cannot be determined by proton NMR spectra analysis alone (Figures S1 and S2). Therefore, each proton was assigned based on the coupling pattern and ^1H - ^1H COSY spectra. All the carbon atoms were assigned with the aid of HSQC experiments and the coupling between fluorine of trifluoromethyl group and C₇, and C₆ with its distinguished quartet pattern and coupling constant. The tertiary carbons assignment was determined with the help of HMBC experiments. In order to determine the position of the allyl substitution, we measured the possible NOE effects between the allyl protons and dimethoxyphenyl group, but the results were not conclusive. The position of the allyl substitution was verified by HMBC experiments. The assignment of these two isomers is listed in Tables 1 and 2. We observed that the H₁₀ proton at the 2-allyl group interacted with C₁₁, C₁₂, and C₃ carbons (Figure S3). On the other hand, the H₁₀ proton at the 1-allyl substitution did not couple with C₃ carbon but interacted with C₁₁, C₁₂, and C₈ carbons (Figure S4). These long-range ^1H - ^{13}C couplings provide direct evidence to support our assignment.

Structural modification of WAY-169916 blocks estrogen receptor binding and fails to influence ER-mediated transcriptional activity

In a previous study we have demonstrated that WAY-169916 (**1**) is a selective activator of the AHR (22). However, WAY-169916 is also a potent selective ligand for the estrogen receptor (31). We hypothesized that alteration of a critical hydroxyl group in the para position of the phenyl ring to a methoxy group on the benzene ring would result in greatly reduced affinity for the ER and enhanced affinity for the AHR. To achieve this goal and to perform a structure-activity study that would focus on making an effective selective AHR ligand, four derivatives of WAY-169916 were synthesized (Figure 1). WAY-169916, SGA 293, 315 and 360 were subjected to an ER α competition assay that measures the ability of a compound to displace a fluorescent ER ligand. Fluoromone bound to the ER tumbles slowly in solution, giving a higher polarization reading (mP). Compounds that compete the fluoromone away from the ER result in free fluoromone that tumbles faster and provides a lower mP value. Non-specific binding effects can be seen by the shift of mP from ER α and fluoromone alone to the addition of 1% DMSO in the reaction (roughly 10% drop in mP). Addition of estradiol (E₂) at higher

concentrations displaces the fluoromone and represents maximum competition (Figure 2A). SGA 293, 315, and 360 show minimal ER α competition at 10 μ M doses, less than that of 1 nM E₂. Only WAY-169916 demonstrated a highly significant level of binding to the ER α . The marginal level of binding observed with SGA 360 was explored further through a dose-response experiment (Figure 2B). SGA 360 failed to exhibit a dose dependent decrease in polarization, with 10 nM and 10 μ M yielding the same level of inhibition. Furthermore, the addition of SGA 360 to the assay in the absence of ER resulted in a modest level of inhibition in the assay (Figure S5). Whether SGA 360 can bind to ER β was also tested, while both WAY-169916 and E₂ exhibited a marked level of binding, SGA 360 failed to bind to ER β (Figure 2C). This would indicate that SGA 360 is not a ligand for the estrogen receptor.

Since SGA 360 is a derivative of a selective ER ligand we wanted to test whether SGA 360 could act as an ER antagonist and block E₂ mediated induction of the progesterone receptor B gene, an ER target gene. MCF-7 cells were treated with E₂ in the presence or absence of SGA 360 for 4 h and the level of progesterone receptor B mRNA assessed. The results indicate that SGA 360 has no statistically significant effect of the induction of progesterone receptor B gene expression (Figure S6).

SGA compounds fail to stimulate AHR-dependent DRE-mediated transcription activity and exhibit antagonist⁴ activity

The ability of the SGA compounds to induce AHR-mediated agonist activity was tested in the HepG2 40/6 cell line, which contains a stably integrated DRE-driven luciferase vector. None of the SGA compounds tested displayed a significant level of reporter activity (Figure 3A). The ability of SGA compounds to induce *CYP1A1* transcription in Hep G2 40/6 cells was also assessed through quantitative PCR (Figure 3B). Interestingly, SGA 293, WAY-169916, and SGA 360 actually repressed constitutive *CYP1A1* expression. In contrast, SGA 315 induced a significant increase in *CYP1A1* mRNA levels, although considerably lower than 10 nM TCDD. Next, the ability of these compounds to antagonize AHR agonist mediated transcriptional activity was assessed using the HepG2 40/6 reporter cell line. In a dose-dependent manner, all SGA compounds were capable of attenuating TCDD-mediated induction of luciferase activity (Figure 3C), with SGA 315 exhibiting the highest level of competition. In the literature, certain AHR ligands have exhibited species selectivity in their ability to behave as AHR agonists (32). If studies are to be performed using these compounds in vivo their ability to regulate AHR activity needs to be explored in rodent cell lines. Therefore, we tested the ability of the SGA compounds to exhibit agonist activity in Hepa 1.1 cells (Figure 4). SGA 315 was capable of inducing significant agonist activity as what was observed in Hep G2 cells. Several of the SGA compounds appear to exhibit antagonistic activity, blocking the ability of an agonist to mediate transactivation of *Cyp1a1*. Such antagonism could occur through three distinct mechanisms, the first being the mediation of AHR/ARNT heterodimer formation and subsequent binding to a DRE, without any increase in gene transcription. The second possibility is that they are not capable of inducing heterodimer formation. The third mechanism is mediating heterodimer formation that fails to bind to a DRE. To examine this issue further an EMSA was performed with the SGA compounds and only SGA 315 was capable to significantly induce AHR binding to a DRE (Figure 5). This would indicate that SGA 293, 294 and 360 are not able to facilitate AHR/ARNT dimerization capable of binding to a DRE.

SGA compounds are direct ligands for the AHR

In order to demonstrate that SGA compounds directly interact with the ligand-binding pocket of the AHR, a competition binding assay was used. This assay utilizes the photoaffinity ligand, 2-azido-3-[¹²⁵I]iodo-7,8-dibenzo-*p*-dioxin, in the presence or absence of a competitor ligand.

⁴An AHR antagonist is an AHR ligand that is not capable of inducing AHR mediated activities.

Each SGA compound tested effectively competed with the photoaffinity ligand (Figure 6). Both SGA 315 and SGA 360 exhibited a much greater ability to compete for AHR binding sites than WAY-169916, suggesting a higher affinity for the AHR relative to the parent compound.

SGA compounds repress cytokine-mediated *SAA1* induction in an AHR dependent manner

We have recently demonstrated that WAY-169916 is capable of repressing *SAA1* induction in Huh7 cells in a AHR-dependent manner (22). Huh7 cells were treated with SGA compounds for 1 h prior to exposure to IL1B for 3 h. Each SGA compound at a 10 μ M concentration was tested in this assay and all were found to repress IL1B-mediated induction of *SAA1* (Figure 6). SGA 315, which exhibits some agonist activity, yielded the greatest level of repression.

The SAhRM SGA360 exhibits anti-inflammatory activity in vivo

The cell culture-based data assessing the anti-inflammatory properties of the putative SAhRM SGA360 clearly suggest the capacity of SGA360 to suppress inflammatory *SAA1* signaling in an AHR-dependent manner through a mechanism that does not require AHR binding to its cognate response element; consequently SGA360 fulfills the criteria of a SAhRM under cell culture conditions. While cell culture data is informative, it is descriptive of the effect in an isolated and homogeneous cell population and may not accurately convey an *in vivo* physiological response. Therefore, we further investigated the anti-inflammatory activity of SGA360 in an *in vivo* murine model of inflammation. The phorbol ester (TPA)-induced ear edema model is a well established model utilized to examine the anti-inflammatory efficacy of test substances and was used here to determine the capacity of SGA360 to suppress inflammatory responses. 6 week old male C57/B6J mice (wild-type or *Ahr*^{-/-}) were exposed to 1.5 μ g TPA or 30 μ g SGA360 in combination with TPA through topical application to the right ear, whilst the left ear received vehicle (acetone) alone. Following 6 h exposure, the degree of TPA-induced inflammation and the effect of SGA360 were assessed by edema quantification and quantitative PCR (Figure 8 and 9). Physical measurement of ear thickness and the wet weight of 7 mm ear punches (Figure 8A) revealed that 6 h topical exposure to 1.5 μ g TPA is sufficient to evoke a marked inflammatory response and subsequent edema. Exposure to SGA360 immediately prior to administration of TPA significantly diminished both of these inflammatory indicators in wild-type mice by ~50 % (Figure 8B). Exposure to SGA360 alone was indistinguishable from vehicle-treated regarding ear thickness and weight (data not shown). Contrary to the anti-inflammatory effect of SGA360 observed in wild-type animals, exposure of *Ahr*^{-/-} animals to SGA360 and TPA revealed no significant decrease in either edema thickness or wet weight thus indicating a requirement for AHR expression to mediate the inhibitory effect of SGA360 on TPA-induced edema. The observed *in vivo* diminishment of physical edema parameters by SGA360 prompted us to examine the effect of SGA360 upon pro-inflammatory gene expression. Using RNA isolated from ear punches taken from animals exposed to vehicle, TPA and SGA360/TPA, the mRNA expression levels of cyclooxygenase-2 (*Cox2*), interleukin 6 (*Il6*), interleukin 1 beta (*Il1b*), serum amyloid-associated-3 (*Saa3*) and interleukin 10 (*Il10*) were examined by quantitative PCR (Figure 9). Exposure of C57BL/6/J mice to TPA for 6 h stimulated the expression of all gene targets examined relative to vehicle-treated controls, consistent with the appearance of edema. Application of SGA360 immediately prior to TPA resulted in a significant suppression of inflammatory gene expression. *Cox2* mRNA was reduced to near basal levels, whilst *Il6*, *Il1b*, *Saa3* and *Il10* were repressed by 70, 70, 90 and 75 %, respectively relative to TPA treatment alone. In contrast, *Ahr*^{-/-} mice under the same treatment regime failed to demonstrate any significant repression of the same inflammatory gene targets relative to TPA-treated alone (Figure 9). Interestingly, with the exception of *Saa3*, the basal and TPA-induced levels of the inflammatory gene targets were lower in *Ahr*^{-/-} mice than in their wild-type counterparts and thus consistent with the slightly diminished onset of edema observed with *Ahr*^{-/-} animals. Such data demonstrates that the

SAhRM SGA360 has *in vivo* anti-inflammatory activity and emphasizes a requirement of AHR to facilitate such potential.

Discussion

There are basically two types of selective nuclear receptor ligands, the first class are ligands that induce receptor dimerization, subsequent binding to their cognate response element and mediate selective recruitment of coactivators/corepressors. The second type of selective ligand induces dimerization but fails to elicit binding to its response element. An example of the latter is the identification of a selective glucocorticoid receptor (GR) ligand (33). The discovery of selective GR ligands (e.g. ZK 216348), in theory, could result in repression of inflammation without many of the side effects of classical GR activators. Studies with the estrogen receptor (ER) have developed highly selective ligands that bind to the receptor and selectively activate nuclear binding to other transcription factors such as NFkB (23). In contrast, these ligands fail to induce estrogen response element driven gene expression or estradiol-mediated physiological effects, such as uterine weight gain (31). One such ER selective ligand, WAY-169916, can effectively inhibit the progression of rheumatoid arthritis in a rat model system and inhibit inflammatory bowel disease in a transgenic rat model (31,34). The same line of reasoning used in these studies was pursued in the development of selective AHR ligands. However, as a bHLH-PAS protein the AHR has a markedly different arrangement of functional domains compared to nuclear receptors, and thus may not be as amenable to being selectively activated. For example, the AF2 transactivation domain and ligand binding pocket are in close proximity in nuclear receptors. In contrast, the transactivation and ligand binding domains appear to be distinct regions in the AHR. Whether the binding of a ligand to the AHR can influence coactivator recruitment or AHR/ARNT DNA-binding is less certain. In a recent study we have shown that WAY-166916 is both a selective estrogen and Ah receptor ligand, with higher affinity for the estrogen receptor (22). A series of studies with WAY-169916 have revealed that it exhibits minimal AHR agonist activity, yet is efficient at repressing acute phase gene expression. WAY-169916 can be classified as a SAhRM, yet its ability to act as a selective ligand for the ER limits its usefulness in terms of studying AHR function. The goal of this study was to develop a derivative of WAY-169916 that fails to bind to the ER and exhibits greater affinity for the AHR. The cocrystal structure of WAY-169916 occupying the estrogen receptor ligand binding pocket reveals that the phenol of WAY-169916 interacts with Glu-353 and Arg-394 and this interaction is believed to be a key component of its high affinity for the estrogen receptor (23). This notion, coupled with the concept that polar groups usually decrease the affinity of ligands for the AHR, lead to examining the effects of substituting methoxy groups for hydroxyl groups in WAY-169916. The replacement of one or two hydroxyl groups with methoxy groups leads to almost total loss of estrogen receptor binding for SGA 315, 293 and 360 (Figure 2). In order to be considered a SAhRM, the SGA compound needed to exhibit a lack of agonist activity in both mouse and human reporter cell lines. Both SGA 293 and SGA 360 would meet this criterion, in contrast SGA 315 and 294 exhibited a statistically significant increase in AHR-mediated reporter activity in cells. Furthermore, SGA 293 and SGA 360 exhibited similar potential to repress cytokine-mediated induction of *SAI1* gene expression. Examination of the relative affinity of each SGA compound in an AHR competition ligand-binding assay revealed that SGA 360 has a higher affinity for the human AHR than SGA 293. This would indicate that the position of the methoxy groups around the phenyl ring has a profound influence on their affinity for the AHR. Nevertheless, both SGA 293 and SGA 360 met the goal of this study to generate useful SAhRMs that fail to interact with the ER.

Cell culture-based studies with Huh7 cells illustrating the suppression of cytokine-mediated inflammatory gene expression (e.g. *SAI1*) by Way-169916 (22,31) and SGA 360 clearly demonstrate the anti-inflammatory potential of SAhRMs. However, cell culture-based observations are limited in that they are restricted to a single homogeneous population and thus

may not accurately reflect physiological responses. Inflammation is a complex process requiring extensive interplay among numerous cell types, thus putative anti-inflammatory modulators require *in vivo* examination. Verification of the anti-inflammatory activity of the SAhRM SGA 360 was demonstrated using the long established TPA-induced ear edema model. Furthermore, *Ahr*^{-/-} animals while responsive to TPA, proved to be refractory to the anti-inflammatory activity of SGA 360, thus implicating AHR in its mode of action. While the parent compound Way-169916 can exert suppressive effects upon inflammatory signaling through ER and AHR (22,31), SGA 360 exhibits minimal ER binding, suggesting that the suppressive action of SGA 360 may be solely mediated through AHR. Pro-inflammatory gene expression (e.g. *Cox2* and *Il1b*) mediated by TPA was markedly repressed by SGA 360. The mechanism of such AHR-dependent repression remains to be elucidated but is likely to involve either protein-protein cross-talk or the ability of a SAhRM to block DRE-mediated AHR activity. While *Cox2* is expressed within the epidermis in response to TPA, the expression of cytokines eg *Il1b* and *Il6* is likely to occur within the epidermis together with resident and infiltrating immune cells. Thus, it is probable that SGA 360 exerts its anti-inflammatory action in multiple cell-types, consistent with previous reports demonstrating a role for AHR in modulating responses to inflammatory stimuli in both skin and immune cells, such as T_H1/2, T_H17, and macrophages (11,14,35,36). It is noteworthy that the efficacy of SGA 360, with regard to inhibition of TPA-induced edematosis, is of the same magnitude as that observed with similar doses of glucocorticoids and non-steroidal anti-inflammatory drugs (37). The inhibition of inflammation by SAhRM ligands is consistent with previous reports demonstrating a role for the high-affinity *Ahr*^{b-1} allele in dampening inflammatory signaling in skin following exposure to pro-inflammatory stimuli (36). Such observations may indicate that the production of endogenous AHR ligands capable of limiting inflammatory responses in a SAhRM-like fashion may be produced *in vivo*. For example, the arachidonic acid derivative, 12(R)-HETE, an activator of AHR can be produced in skin during inflammation, and thus could contribute to the regulation of AHR activity in skin cells (38). Interestingly, sustained activation of AHR in keratinocytes promotes inflammatory signaling in mice (39). The contradictory nature of AHR activity is likely to involve inflammatory cytokines (e.g. IL-6, IL-18 and CCL20), which have a DRE-mediated regulatory component (39,40), and results in elevated expression in response to potent AHR agonists or heightened AHR protein levels. Although these cytokines were not examined in the context of SGA 360 exposure, the inhibition of DRE binding by SAhRMs similar to SGA 360 is likely to suppress such activity and further contribute to its anti-inflammatory profile.

When considering regulation of AHR-mediated modulation of transcription, it is important to clearly understand differences between a SAhRM and an AHR antagonist and their possible differences in activity, in a particular biological context. For example, if one is interested in blocking a DRE-mediated event such as the induction of *CYP1A1*, both an antagonist and a SAhRM will exhibit the same apparent inhibitory activity. If the goal were to block all direct AHR-mediated transcriptional modulatory events, an AHR antagonist and a SAhRM would yield very different results. Interestingly, an AHR antagonist is defined in the literature as an AHR ligand that fails to induce a DRE-mediated enhancement of gene expression. This is due to the fact that the AHR was only recently shown to repress gene transcription through protein-protein interactions (20,41). Thus, whether previously described AHR antagonists are pure antagonists or SAhRMs will require further investigation. An example of these concepts is the activity of α -naphthoflavone (α -NF), which is considered a partial agonist/antagonist and is often used as an antagonist to a full agonist such as TCDD. This flavonoid exhibits a modest ability to induce *CYP1A1* mRNA yet is similar to TCDD in its ability, at a relatively high concentration, to inhibit *SAA3* expression after cytokine exposure (20). Thus, α -NF exhibits partial agonist/antagonist activity, yet is capable of exhibiting full repression potential.

The potential importance of developing SAhRMs or AHR antagonists is becoming increasingly apparent. At least three specific physiologically important targets modulated by AHR activity have emerged. The first is the ability of the AHR to modulate T cell differentiation, and in particular, their differentiation into T_H17 cells and an IL22 producing T cell subpopulation that is important in skin (14,42). Studies in cell culture reveal that an AHR antagonist can impair T_H17 cell development, suggesting that an AHR antagonist could have therapeutic potential in treating chronic inflammatory diseases (15). The AHR can repress expression of acute-phase genes, which can be continuously up-regulated during chronic inflammatory diseases such as rheumatoid arthritis. Excessive production of acute phase gene products such as SAA can lead to enhanced inflammation and amyloidosis, thus attenuation of the acute phase response in liver would be a second therapeutic target that can be altered by selective activation or antagonism of the AHR. The third possible target is the ability of a SAhRM to inhibit estrogenic activity in breast cancer (43). Most likely, if each of these relevant target diseases were to be treated with an AHR ligand, a SAhRM would be the most logical choice, as an AHR agonist will also modulate DRE-driven AHR transcriptional activity that could lead to toxicity or alter drug metabolism. Future studies are needed to test whether SGA 360 would be effective in treating chronic inflammatory diseases.

Supplementary Material

Refer to Web version on PubMed Central for supplementary material.

Acknowledgments

We thank Dr. Michael Denison for H1L1.1c2 cells and Kelly Wagner for her technical assistance for the SAA repression assay. We thank Marcia H. Perdew for editorial assistance. This work was supported by NIEHS, National Institutes of Health Grants ES04869. The NMR instrumentation in this project is funded, in part, under a grant from the Pennsylvania Department of Health using Tobacco Settlement Funds. The Department specifically disclaims responsibility for any analyses, interpretations or conclusions. Additional instrumentation support came from NIH 1 S10 RR021172.

Abbreviations

TNFA	tumor necrosis factor- α
IL1B	interleukin 1 β
SAA	serum amyloid A
NFKB	nuclear factor- κ B
AHR	Ah receptor
ARNT	AHR nuclear translocator
DRE	dioxin responsive element
CYP1A1	cytochrome P450 1A1
T _H 1 or T _H 2	T lymphocyte helper type 1 and 2
SAhRM	selective AHR modulator
ER	estrogen receptor
THF	tetrahydrofuran
DMSO	dimethyl sulfoxide
TPA	12-O-tetradecanoylphorbol-13-acetate
E ₂	estradiol

TCDD	2,3,7,8-tetrachlorodibenzo- <i>p</i> -dioxin
GR	glucocorticoid receptor
α -NF	α -naphthoflavone.

References

- (1). Gabay C, Kushner I. Acute-phase proteins and other systemic responses to inflammation. *N Engl J Med* 1999;340:448–454. [PubMed: 9971870]
- (2). Cheng N, He R, Tian J, Ye PP, Ye RD. Cutting edge: TLR2 is a functional receptor for acute-phase serum amyloid A. *J Immunol* 2008;181:22–26. [PubMed: 18566366]
- (3). Okamoto H, Katagiri Y, Kiire A, Momohara S, Kamatani N. Serum amyloid A activates nuclear factor-kappaB in rheumatoid synovial fibroblasts through binding to receptor of advanced glycation end-products. *J Rheumatol* 2008;35:752–756. [PubMed: 18322992]
- (4). Lee MS, Yoo SA, Cho CS, Suh PG, Kim WU, Ryu SH. Serum amyloid A binding to formyl peptide receptor-like 1 induces synovial hyperplasia and angiogenesis. *J Immunol* 2006;177:5585–5594. [PubMed: 17015746]
- (5). Yan SD, Zhu H, Zhu A, Golabek A, Du H, Roher A, Yu J, Soto C, Schmidt AM, Stern D, Kindy M. Receptor-dependent cell stress and amyloid accumulation in systemic amyloidosis. *Nat Med* 2000;6:643–651. [PubMed: 10835680]
- (6). Beischlag TV, Luis Morales J, Hollingshead BD, Perdew GH. The aryl hydrocarbon receptor complex and the control of gene expression. *Crit Rev Eukaryot Gene Expr* 2008;18:207–250. [PubMed: 18540824]
- (7). McMillan BJ, Bradfield CA. The aryl hydrocarbon receptor sans xenobiotics: endogenous function in genetic model systems. *Mol Pharmacol* 2007;72:487–498. [PubMed: 17535977]
- (8). Baba T, Mimura J, Nakamura N, Harada N, Yamamoto M, Morohashi K, Fujii-Kuriyama Y. Intrinsic function of the aryl hydrocarbon (dioxin) receptor as a key factor in female reproduction. *Mol Cell Biol* 2005;25:10040–10051. [PubMed: 16260617]
- (9). Barnett KR, Tomic D, Gupta RK, Miller KP, Meachum S, Paulose T, Flaws JA. The aryl hydrocarbon receptor affects mouse ovarian follicle growth via mechanisms involving estradiol regulation and responsiveness. *Biol Reprod* 2007;76:1062–1070. [PubMed: 17329597]
- (10). Lund AK, Agbor LN, Zhang N, Baker A, Zhao H, Fink GD, Kanagy NL, Walker MK. Loss of the aryl hydrocarbon receptor induces hypoxemia, endothelin-1, and systemic hypertension at modest altitude. *Hypertension* 2008;51:803–809. [PubMed: 18212270]
- (11). Negishi T, Kato Y, Ooneda O, Mimura J, Takada T, Mochizuki H, Yamamoto M, Fujii-Kuriyama Y, Furusako S. Effects of aryl hydrocarbon receptor signaling on the modulation of TH1/TH2 balance. *J Immunol* 2005;175:7348–7356. [PubMed: 16301641]
- (12). Morales JL, Krzeminski J, Amin S, Perdew GH. Characterization of the antiallergic drugs 3-[2-(2-phenylethyl) benzoimidazole-4-yl]-3-hydroxypropanoic acid and ethyl 3-hydroxy-3-[2-(2-phenylethyl)benzoimidazol-4-yl]propanoate as full aryl hydrocarbon receptor agonists. *Chem Res Toxicol* 2008;21:472–482. [PubMed: 18179178]
- (13). Peck A, Mellins ED. Breaking old paradigms: Th17 cells in autoimmune arthritis. *Clin Immunol*. 2009
- (14). Veldhoen M, Hirota K, Westendorf AM, Buer J, Dumoutier L, Renauld JC, Stockinger B. The aryl hydrocarbon receptor links TH17-cell-mediated autoimmunity to environmental toxins. *Nature* 2008;453:106–109. [PubMed: 18362914]
- (15). Veldhoen M, Hirota K, Christensen J, O'Garra A, Stockinger B. Natural agonists for aryl hydrocarbon receptor in culture medium are essential for optimal differentiation of Th17 T cells. *J Exp Med* 2009;206:43–49. [PubMed: 19114668]
- (16). Kimura A, Naka T, Nohara K, Fujii-Kuriyama Y, Kishimoto T. Aryl hydrocarbon receptor regulates Stat1 activation and participates in the development of Th17 cells. *Proc Natl Acad Sci U S A* 2008;105:9721–9726. [PubMed: 18607004]

- (17). Kitamura M, Kasai A. Cigarette smoke as a trigger for the dioxin receptor-mediated signaling pathway. *Cancer Lett* 2007;252:184–194. [PubMed: 17189671]
- (18). Tian Y, Ke S, Denison MS, Rabson AB, Gallo MA. Ah receptor and NF-kappaB interactions, a potential mechanism for dioxin toxicity. *J Biol Chem* 1999;274:510–515. [PubMed: 9867872]
- (19). Jensen BA, Leeman RJ, Schlezinger JJ, Sherr DH. Aryl hydrocarbon receptor (AhR) agonists suppress interleukin-6 expression by bone marrow stromal cells: an immunotoxicology study. *Environ Health* 2003;2:16. [PubMed: 14678569]
- (20). Patel RD, Murray IA, Flaveny CA, Kusradi A, Perdew GH. Ah receptor represses acute-phase response gene expression without binding to its cognate response element. *Lab Invest* 2009;89:695–707. [PubMed: 19333233]
- (21). Bunger MK, Glover E, Moran SM, Walisser JA, Lahvis GP, Hsu EL, Bradfield CA. Abnormal liver development and resistance to 2,3,7,8-tetrachlorodibenzo-p-dioxin toxicity in mice carrying a mutation in the DNA-binding domain of the aryl hydrocarbon receptor. *Toxicol Sci* 2008;106:83–92. [PubMed: 18660548]
- (22). Murray IA, Morales JL, Flaveny CA, Dinatale BC, Chiaro C, Gowdahalli K, Amin S, Perdew GH. Evidence for ligand-mediated selective modulation of aryl hydrocarbon receptor activity. *Mol Pharmacol* 2010;77:247–254. [PubMed: 19903824]
- (23). Steffan RJ, Matelan E, Ashwell MA, Moore WJ, Solvibile WR, Trybulski E, Chadwick CC, Chippari S, Kenney T, Eckert A, Borges-Marcucci L, Keith JC, Xu Z, Mosyak L, Harnish DC. Synthesis and activity of substituted 4-(indazol-3-yl)phenols as pathway-selective estrogen receptor ligands useful in the treatment of rheumatoid arthritis. *J Med Chem* 2004;47:6435–6438. [PubMed: 15588074]
- (24). Long WP, Pray-Grant M, Tsai JC, Perdew GH. Protein kinase C activity is required for aryl hydrocarbon receptor pathway-mediated signal transduction. *Mol Pharmacol* 1998;53:691–700. [PubMed: 9547360]
- (25). Garrison PM, Tullis K, Aarts JM, Brouwer A, Giesy JP, Denison MS. Species-specific recombinant cell lines as bioassay systems for the detection of 2,3,7,8-tetrachlorodibenzo-p-dioxin-like chemicals. *Fundam Appl Toxicol* 1996;30:194–203. [PubMed: 8812265]
- (26). Poland A, Glover E, Ebetino H, Kende A. Photoaffinity labelling of the Ah receptor. *Food Chem Toxicol* 1986;24:781–787. [PubMed: 3023216]
- (27). Ramadoss P, Perdew GH. Use of 2-azido-3-[125I]iodo-7,8-dibromodibenzo-p-dioxin as a probe to determine the relative ligand affinity of human versus mouse aryl hydrocarbon receptor in cultured cells. *Mol Pharmacol* 2004;66:129–136. [PubMed: 15213304]
- (28). Flaveny CA, Murray IA, Chiaro CR, Perdew GH. Ligand selectivity and gene regulation by the human aryl hydrocarbon receptor in transgenic mice. *Mol Pharmacol* 2009;75:1412–1420. [PubMed: 19299563]
- (29). Nahm S, Weinreb SM. N-methoxy-N-methylamides as effective acylating agents. *Tetrahedron Lett* 1981;22:3815–3818.
- (30). De Luca L, Giacomelli G, Taddei M. An easy and convenient synthesis of Weinreb amides and hydroxamates. *J Org Chem* 2001;66:2534–2537. [PubMed: 11281806]
- (31). Chadwick CC, Chippari S, Matelan E, Borges-Marcucci L, Eckert AM, Keith JC Jr. Albert LM, Leathurby Y, Harris HA, Bhat RA, Ashwell M, Trybulski E, Winneker RC, Adelman SJ, Steffan RJ, Harnish DC. Identification of pathway-selective estrogen receptor ligands that inhibit NF-kappaB transcriptional activity. *Proc Natl Acad Sci U S A* 2005;102:2543–2548. [PubMed: 15699342]
- (32). Zhang S, Qin C, Safe SH. Flavonoids as aryl hydrocarbon receptor agonists/antagonists: effects of structure and cell context. *Environ Health Perspect* 2003;111:1877–1882. [PubMed: 14644660]
- (33). Schacke H, Schottelius A, Docke WD, Strehlke P, Jaroch S, Schmees N, Rehwinkel H, Hennekes H, Asadullah K. Dissociation of transactivation from transrepression by a selective glucocorticoid receptor agonist leads to separation of therapeutic effects from side effects. *Proc Natl Acad Sci U S A* 2004;101:227–232. [PubMed: 14694204]
- (34). Keith JC Jr. Albert LM, Leathurby Y, Follettie M, Wang L, Borges-Marcucci L, Chadwick CC, Steffan RJ, Harnish DC. The utility of pathway selective estrogen receptor ligands that inhibit nuclear factor-kappa B transcriptional activity in models of rheumatoid arthritis. *Arthritis Res Ther* 2005;7:R427–438. [PubMed: 15899029]

- (35). Shi LZ, Faith NG, Nakayama Y, Suresh M, Steinberg H, Czuprynski CJ. The aryl hydrocarbon receptor is required for optimal resistance to *Listeria monocytogenes* infection in mice. *J Immunol* 2007;179:6952–6962. [PubMed: 17982086]
- (36). De Souza VR, Cabrera WK, Galvan A, Ribeiro OG, De Franco M, Vorraro F, Starobinas N, Massa S, Dragani TA, Ibanez OM. Aryl hydrocarbon receptor polymorphism modulates DMBA-induced inflammation and carcinogenesis in phenotypically selected mice. *Int J Cancer* 2009;124:1478–1482. [PubMed: 19065662]
- (37). De Young LM, Kheifets JB, Ballaron SJ, Young JM. Edema and cell infiltration in the phorbol ester-treated mouse ear are temporally separate and can be differentially modulated by pharmacologic agents. *Agents Actions* 1989;26:335–341. [PubMed: 2567568]
- (38). Chiaro CR, Patel RD, Perdew GH. 12(R)-Hydroxy-5(Z),8(Z),10(E),14(Z)-eicosatetraenoic acid [12(R)-HETE], an arachidonic acid derivative, is an activator of the aryl hydrocarbon receptor. *Mol Pharmacol* 2008;74:1649–1656. [PubMed: 18779363]
- (39). Tauchi M, Hida A, Negishi T, Katsuoka F, Noda S, Mimura J, Hosoya T, Yanaka A, Aburatani H, Fujii-Kuriyama Y, Motohashi H, Yamamoto M. Constitutive expression of aryl hydrocarbon receptor in keratinocytes causes inflammatory skin lesions. *Mol Cell Biol* 2005;25:9360–9368. [PubMed: 16227587]
- (40). Hollingshead BD, Beischlag TV, Dinatale BC, Ramadoss P, Perdew GH. Inflammatory signaling and aryl hydrocarbon receptor mediate synergistic induction of interleukin 6 in MCF-7 cells. *Cancer Res* 2008;68:3609–3617. [PubMed: 18483242]
- (41). Beischlag TV, Perdew GH. ER alpha-AHR-ARNT protein-protein interactions mediate estradiol-dependent transrepression of dioxin-inducible gene transcription. *J Biol Chem* 2005;280:21607–21611. [PubMed: 15837795]
- (42). Trifari S, Kaplan CD, Tran EH, Crellin NK, Spits H. Identification of a human helper T cell population that has abundant production of interleukin 22 and is distinct from T(H)-17, T(H)1 and T(H)2 cells. *Nat Immunol* 2009;10:864–871. [PubMed: 19578368]
- (43). Zhang S, Lei P, Liu X, Li X, Walker K, Kotha L, Rowlands C, Safe S. The aryl hydrocarbon receptor as a target for estrogen receptor-negative breast cancer chemotherapy. *Endocr Relat Cancer* 2009;16:835–844. [PubMed: 19447902]

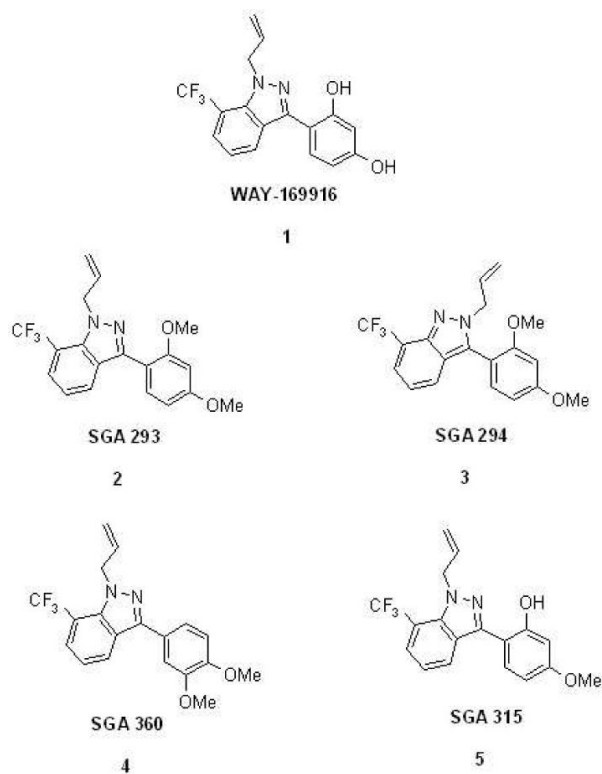
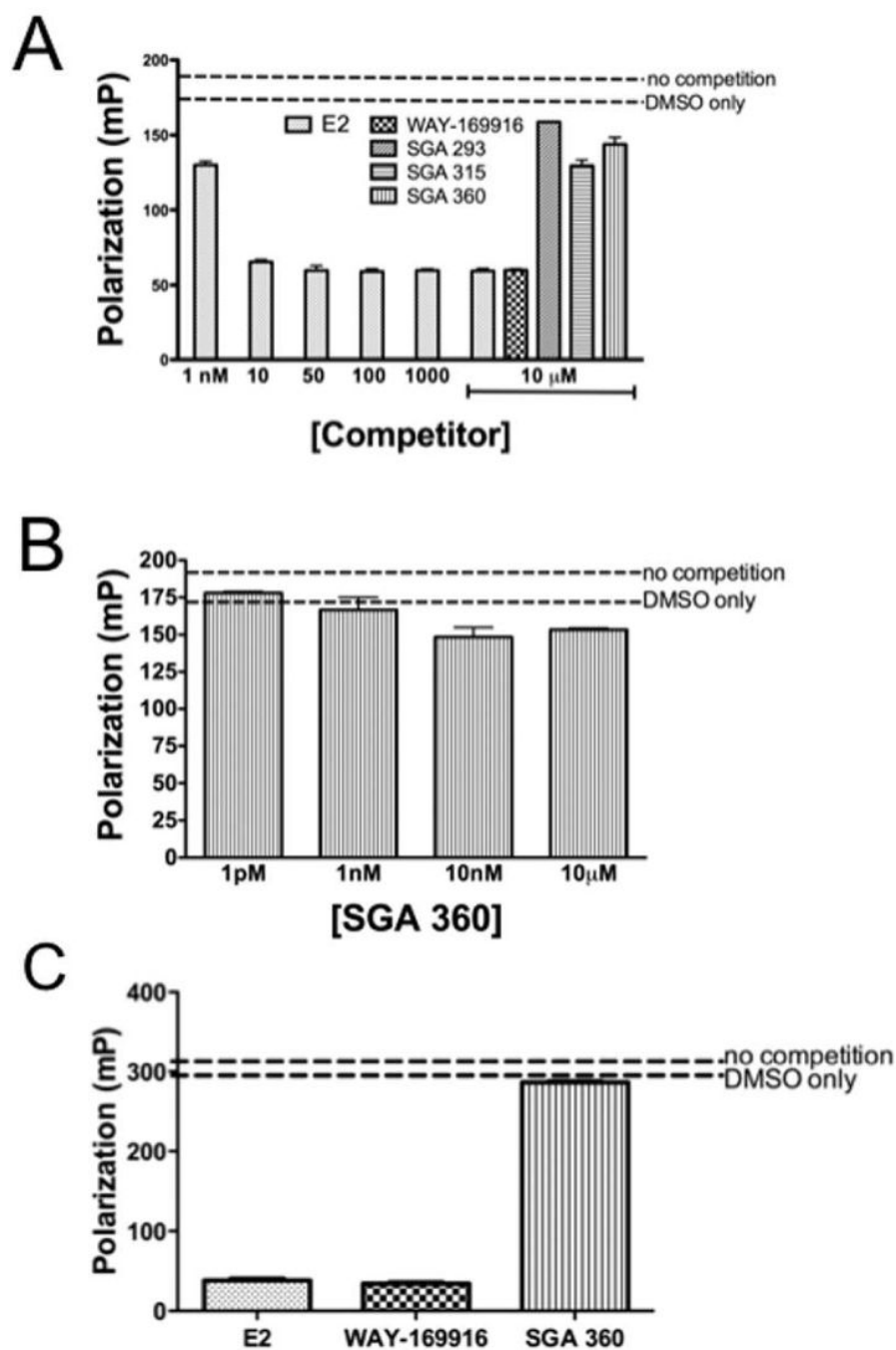


Figure 1. Structures of indazole derivatives; compound **1** (WAY-169916); **2** (SGA 293); **3** (SGA 294); **4** (SGA 360); and **5** (SGA 315).

**Figure 2.**

Structural modification of WAY-169916 blocks binding to the estrogen receptor. (A) Estrogen receptor α fluorescence polarization assays were performed on each SGA compound. (B) A dose-response Estrogen receptor α fluorescence polarization assay experiment was performed on SGA 360. (C) Estrogen receptor β fluorescence polarization assays were performed.

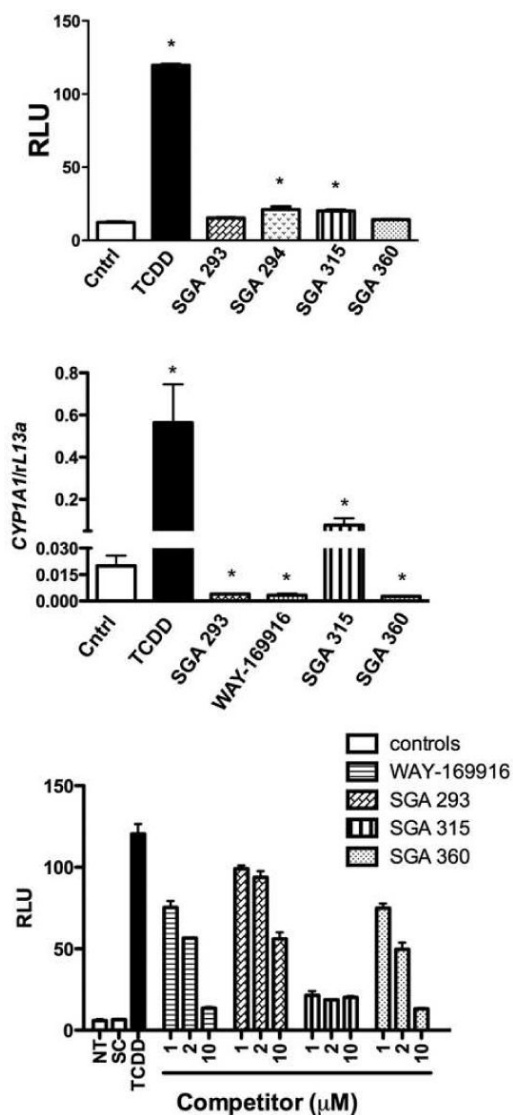


Figure 3.

Assessment of AHR agonist or antagonist transcriptional activity in human cells mediated by the SGA compounds. (A) HepG2 40/6 stable reporter cell line was treated with 2 nM TCDD or 10 μM of each SGA compound for 4 h, cells were lysed and DRE-driven luciferase activity determined. (B) HepG2 40/6 cells were treated as indicated for 4 h, RNA was isolated, *CYP1A1* and *rL13a* mRNA levels were determined using real-time RT-PCR. (C) Co-treatment of HepG2 40/6 cells with SGA compounds and 2 nM TCDD for 4 h followed by measurement of luciferase activity. Data represent mean ± SEM. Statistically significant changes that are marked with an asterisk are relative to control ($n = 3/\text{treatment group}$; * $P < 0.05$).

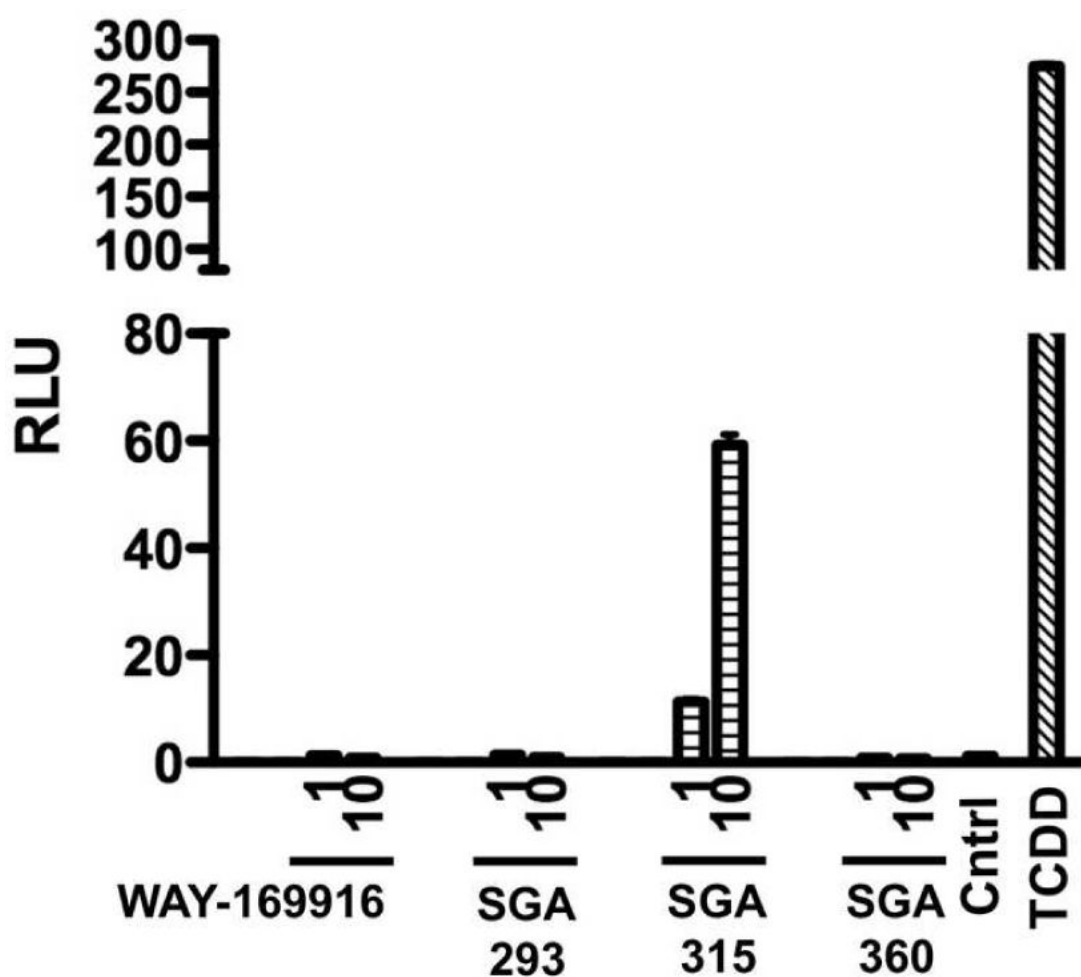


Figure 4.

Assessment of AHR-driven transcriptional activity in a mouse reporter cell line mediated by the SGA compounds. H1L1.1c2 cells were treated with 1 nM TCDD or 10 μM of each SGA compound for 4 h, cells were lysed and DRE-driven luciferase activity determined.

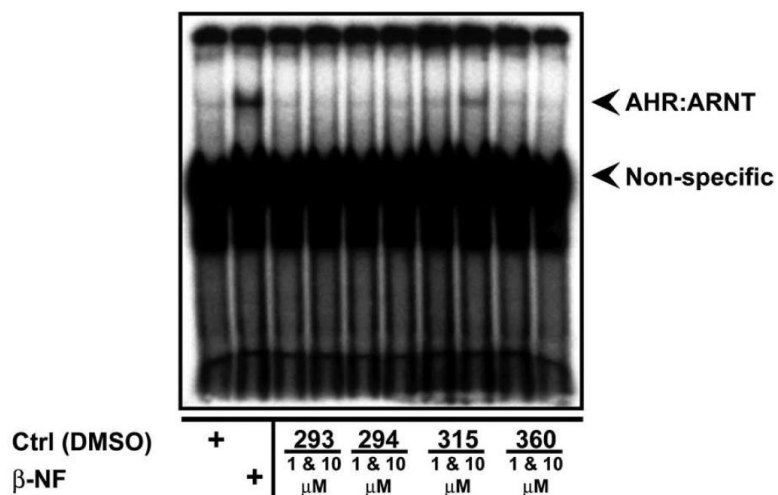


Figure 5. SGA 315 is capable of activating AHR/ARNT DNA binding in an EMSA. Each SGA compound was tested for its ability to induce AHR/ARNT binding to a DRE containing oligonucleotide. The AHR agonist β-naphthoflavone (β-NF) was utilized as a positive control.

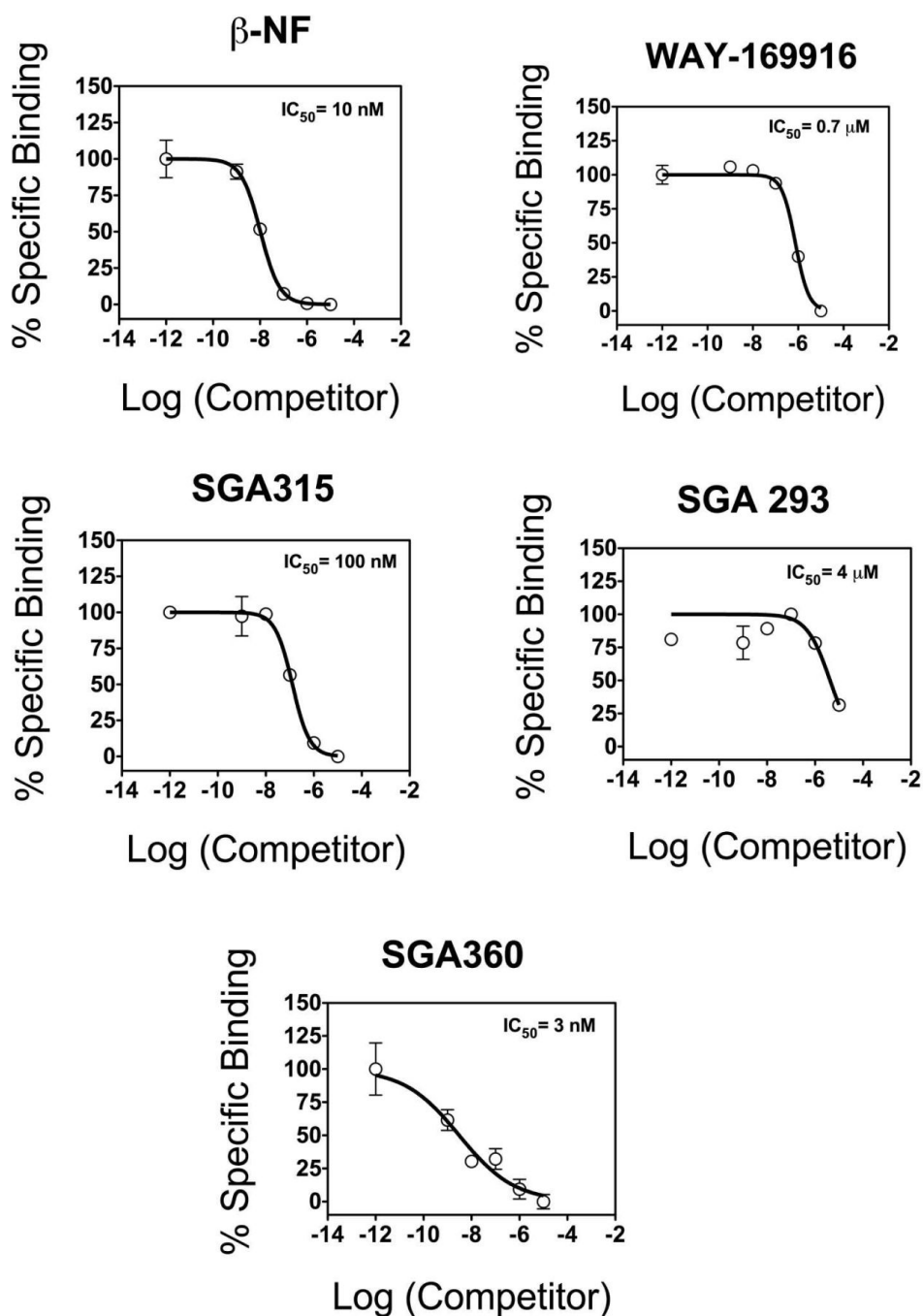


Figure 6.

SGA compounds vary in their ability to compete with the photoaffinity ligand in a competition AHR binding assay. Increasing amounts of the compounds labeled in each graph were added to mouse liver cytosol expressing the human AHR in the presence of the photoaffinity ligand (420 pM). After exposure to UV light, samples were subjected to tricine SDS-PAGE, transferred to membrane and radioactive bands were excised and counted in a γ counter.

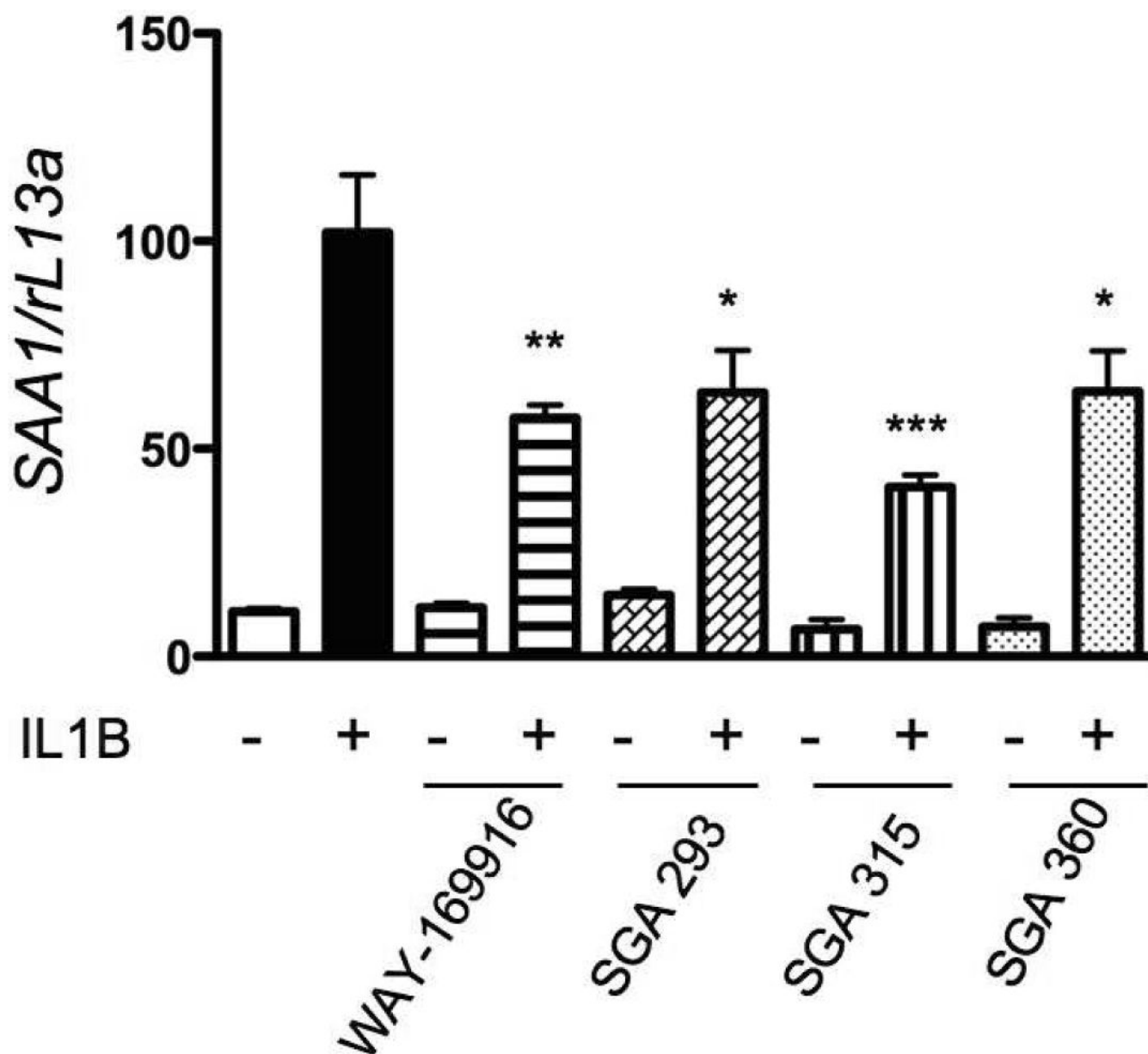


Figure 7.

All of the SGA compounds are able to inhibit IL1B-mediated *SAA1* gene expression. Huh7 cells were pretreated with each SGA compound for 1 h prior to the addition of 2 ng/ml IL1B. After 3 h RNA was isolated and the level of *SAA1* and *rL13a* mRNA determined. Data represent mean \pm SEM. Statistically significant changes that are marked with an asterisk are relative to IL1B treatment alone ($n = 3$ /treatment group; * $P < 0.05$; ** $P < 0.01$; *** $P < 0.001$).

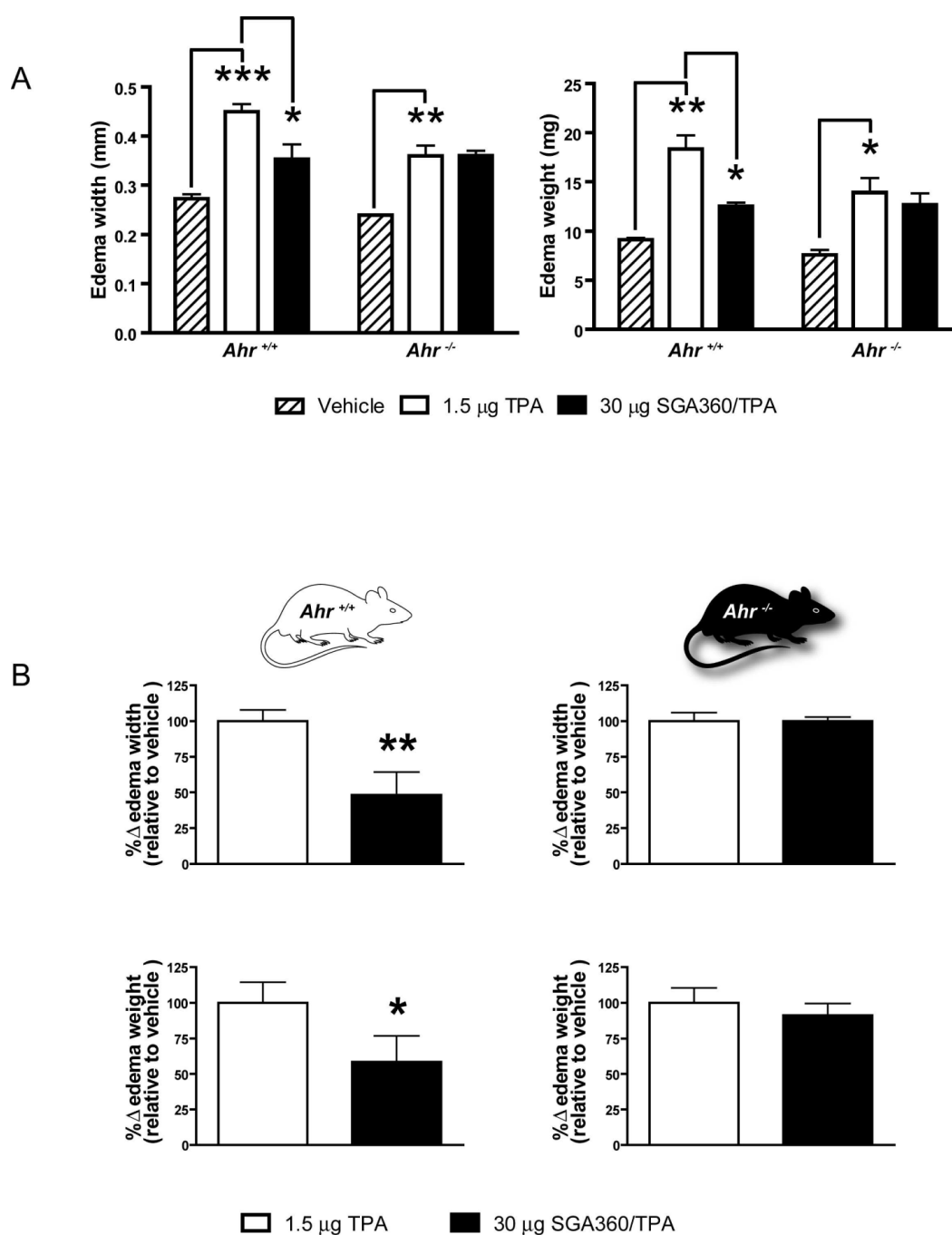


Figure 8. SGA360 exhibits anti-inflammatory properties in vivo

Ear inflammation was induced in anesthetized 6-week-old male C57/B6J mice (wild-type or *Ahr*^{-/-}) through topical application of 1.5 µg TPA in 50 µl vehicle (acetone) to the right ear. Anti-inflammatory properties of SGA360 were examined through topical application of 30 µg SGA360 in 50 µl vehicle immediately followed by administration of TPA. In all cases the left ear received vehicle alone. The degree of inflammation was assessed after 6 h by measuring ear edema thickness using a micrometer and ear edema wet weight following removal of 7 mm diameter ear punch. Data represent (A) mean edema thickness (mm) and mean edema weight (mg) ± SEM. (B) Mean percentage change in edema thickness and weight relative to vehicle-treated ± SEM. (*n* = 3/treatment group; * *P* < 0.05; ** *P* < 0.01; *** *P* < 0.001).

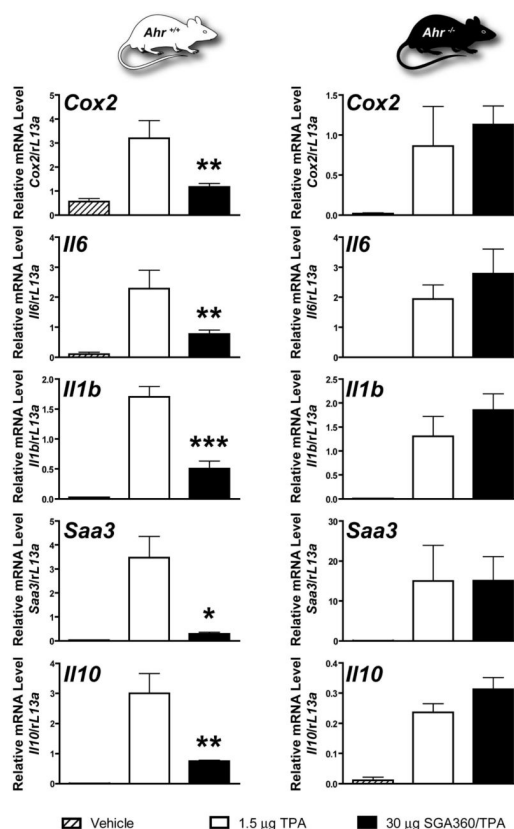
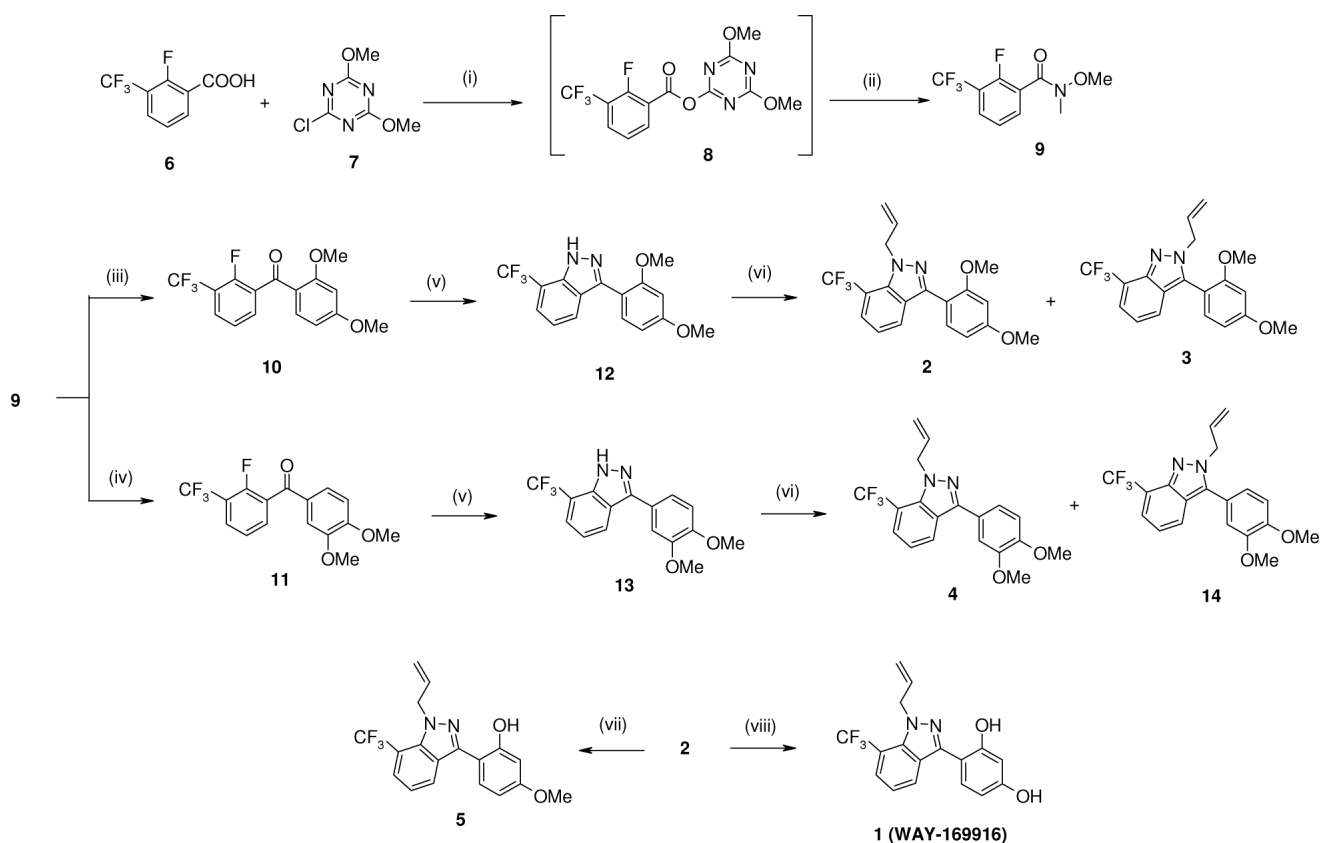


Figure 9. SGA 360 suppressed inflammatory gene expression in vivo

Ear inflammation was induced in anesthetized 6-week-old male C57/B6J mice (wild-type or *Ahr*^{-/-}) through topical application of 1.5 µg TPA in 50 µl vehicle (acetone) to the right ear. Anti-inflammatory properties of SGA 360 were examined through topical application of 30 µg SGA 360 in 50 µl vehicle prior to administration of TPA. In all cases the left ear received vehicle alone. Changes in inflammatory gene expression were assessed through quantitative PCR using primers targeted against *Cox2*, *Il6*, *Il1b*, *Saa3* and *Il10*. Data represent mean mRNA levels normalized to constitutive ribosomal protein *L13* mRNA expression \pm SEM. ($n = 3$ /treatment group; * $P < 0.05$; ** $P < 0.01$; *** $P < 0.001$).

**Scheme 1.**

Synthesis of indazole derivatives.

Reagents and conditions: (i) *N*-methylmorpholine, THF, RT, 1 h (ii) *N,O*-dimethylhydroxylamine hydrochloride, RT, 8 h (iii) 2,4-dimethoxyphenylmagnesium bromide, THF, 0 °C, 2 h, (iv) 3,4-dimethoxyphenylmagnesium bromide, THF, 0 °C, 2 h, (v) anhydrous H₂NNH₂, pyridine, microwave, 250W, 100 °C, 1 h (vi) NaH, DMF, RT to 60 °C, 30 min., allyl bromide, 60 °C, 4 h, (vii) 1 eq. BBr₃, CH₂Cl₂/cyclohexane, -60 °C to RT, 5 h, (viii) 1 eq. BBr₃, CH₂Cl₂/cyclohexane, -60 °C to RT, 5 h.

Table 1
¹H and ¹³C Assignments of 1-allyl-3-(3,4-dimethoxyphenyl)-7-(trifluoromethyl)-1H-indazole.

Proton Assignment			Carbon-13 Assignment		
Proton ^a	Chemical Shift δ:ppm	Multi.	Coupling Constant	C-13 ^b	Coupling Constant
H ₃	N/A	N/A	N/A	C ₃	δ:ppm
H ₄	8.19	d, 1H	J=7.40 Hz	C ₄	124.8
H ₅	7.28	t, 1H	J=7.40 Hz	C ₅	125.35
H ₆	7.79	d, 1H	J=7.40 Hz	C ₆	119.69
				C ₇	125.42
				C ₈	q, J=6.16Hz
				C ₉	q, J=32.75 Hz
				CF ₃	136.32
					145.62
					123.95
					q, J=272.09Hz
Allyl Group					
H ₁₀	5.25	br d, 2H	J=5.12 Hz	C ₁₀	53.45
H ₁₁	6.17–6.09	m, 1H		C ₁₁	133.48
H ₁₂	5.21	dd, 1H	J=10.5 Hz; J=1.3 Hz;	C ₁₂	116.9
H _{12'}	5.07	dd, 1H	J=17.3 Hz; J=1.3 Hz		
Phenyl Group					
H _{1'}	N/A	N/A	N/A	C _{1'}	124.61
H ₂	7.44	d, 1H	J=1.95 Hz	C _{2'}	111.11
H ₃	N/A	N/A	N/A	C _{3'}	149.48
H _{4'}	N/A	N/A	N/A	C _{4'}	149.39
H ₅	7.04	d, 1H	J=8.05 Hz	C _{5'}	111.34
H ₆	7.45	dd, 1H	J=8.05 Hz; J=1.95 Hz	C _{6'}	120.61
3'-OMe	3.99	s, 3H		3'-OMe	56.02
4'-OMe	4.01	s, 3H		4'-OMe	56.06

^aProton NMR was measure at 500 MHz with CDCl₃ as solvent.

¹³C NMR was measure at 125 MHz with CDCl₃ as solvent.

Table 2

¹H and ¹³C Assignments of 2-allyl-3-(3,4-dimethoxyphenyl)-7-(trifluoromethyl)-1H-indazole.

Proton Assignment				Carbon-13 Assignment		
Proton ^a	Chemical Shift δ:ppm	Multi.	Coupling Constant	C-13 ^b	Chemical Shift δ:ppm	Coupling Constant
H ₃	N/A	N/A	N/A	C ₃	137.03	
H ₄	7.78	d, 1H	J=8.33 Hz	C ₄	125.05	
H ₅	7.14	br t, 1H	J=7.76 Hz	C ₅	120.09	
H ₆	7.66	dt, 1H	J=7.04 Hz; J=0.90 Hz	C ₆	124.63	q, J=5.19Hz
				C ₇	118.57	q, J=32.7Hz
				C ₈	143.5	
				C ₉	122.5	
				CF ₃	124.06	q, J=273.5Hz
Allyl Group						
H ₁₀	5.12	dt, 2H	J=5.03 Hz; J=1.53 Hz	C ¹⁰	53.49	
H ₁₁	6.23–6.15	m, 1H		C ₁₁	133.43	
H ₁₂	5.28	dq, 1H	J=10.29 Hz; J=1.02 Hz	C ₁₂	117.9	
H _{12'}	5.06	dq, 1H	J=17.29 Hz; J=1.31 Hz			
Phenyl Group						
H _{1'}	N/A	N/A	N/A	C _{1'}	121.21	
H _{2'}	7.03	d, 1H	J=1.9 Hz	C _{2'}	112.57	
H _{3'}	N/A	N/A	N/A	C _{3'}	149.94	
H _{4'}	N/A	N/A	N/A	C _{4'}	149.28	
H _{5'}	7.07	dd, 1H	J=8.35 Hz; J=1.9 Hz	C _{5'}	111.48	
H _{6'}	7.11	d, 1H	J=8.35 Hz; J=1.9 Hz	C _{6'}	122.56	
3'-OMe	3.93	s, 3H		3'-OMe	56.04	
4'-OMe	4.00	s, 3H		4'-OMe	56.09	

^aProton NMR was measure at 500 MHz with CDCl₃ as solvent.

¹³C NMR was measure at 125 MHz with CDCl₃ as solvent.